SLAC-PUB--5312

DE90 016678

SLAC-PUB-5312
August 1990
(T/E)

BOUND-STATE QUARK AND GLUON CONTRIBUTIONS TO STRUCTURE FUNCTIONS IN QCD*

Stanley J. BRODSKY

Stanford Linear Accelerator Center,
Stanford University, Stanford, California 94309

One can distinguish two types of contributions to the quark and gluon structure functions of hadrons in quantum chromodynamics: "intrinsic" contributions, which are due to the direct scattering on the bound-state constituents, and "extrinsic" contributions, which are derived from particles created in the collision. In this talk, I discuss several aspects of deep inelastic structure functions in which the bound-state structure of the proton plays a crucial role: (1) the properties of the intrinsic gluon distribution associated with the proton bound-state wavefunction; (2) the separation of the quark structure function of the proton into intrinsic "bound-valence" and extrinsic "non-valence" components which takes into account the Pauli principle; (3) the properties and identification of intrinsic heavy quark structure functions; and (4) a theory of shadowing and anti-shadowing of nuclear structure functions, directly related to quark-nucleon interactions and the gluon saturation phenomenon.

1. INTRODUCTION

The main focus of HERA physics will be the measurements of the quark and gluon structure of the proton. Even at the very small values of x_{Bj} which can be probed at HERA, the QCD predictions for structure functions still depend strongly on the input quark and gluon distributions associated with the bound-state structure of the proton.

In this talk I will distinguish two separate contributions to deep inelastic lepton-proton scattering: *intrinsic* (bound-state) and *extrinsic* structure functions. The extrinsic contributions are created by the virtual strong interactions of the lepton and would be present even if the quark fields of the proton were charge-less. The intrinsic bound-valence quark contributions are due to the electron scattering on the quarks described by the proton wavefunction; a complete calculation of these contributions would require solving the bound state problem in QCD. As I shall discuss here, both the Pomeron and leading Reggeon contributions are absent in the bound valence-quark distributions. The leading Regge contributions are thus associated with particles created by the photon-hadron scattering reaction, processes extrinsic to the bound state physics of the target hadron itself.

Despite our confidence that QCD is the correct theory of strong interactions, there are very few definitive theoretical predictions for the non-perturbative bound state quark and gluon distributions which can be directly derived from the theory, although some constraints on the non-perturbative structure of the proton have been obtained using bag models, quark-diquark schemes, QCD sum rules, non-relativistic quark models, and lattice gauge theory.

One new approach, Discretized Light-Cone Quantization,[1] has recently been proposed as a possible way to compute non-perturbative structure functions in gauge theory. In this method one attempts to numerically diagonalize the QCD Hamiltonian quantized on the light-front in light-cone gauge. One chooses as a basis a complete set of discrete momentum-space color-singlet free gluon and quark Hamiltonian Fock states satisfying periodic and anti-periodic boundary conditions, respec-

* Work supported in by the Department of Energy contract DE-AC03-76SF00515.

Invited Talk, Presented at the DESY Topical Meeting: Small-x Behavior of Deep Inelastic Structure Functions in QCD, Hamburg, Germany, May 14-16, 1990.

tively. In principle, the eigenvalues of the full Hamiltonian provide the entire invariant mass spectrum and the corresponding eigenfunctions provide the structure functions and distribution amplitudes needed for QCD factorization formulas. Thus far, the main success of DLCQ has been applications to gauge theories in one-space and one-time dimensions.[1] For example, the spectrum and structure functions of mesons, baryons, and nuclei in QCD(1+1) for $SU(3)_C$ have been obtained as a function of mass and coupling constant. Results for the structure function of the lowest mass meson and baryon at weak and strong coupling are shown in Fig. 1.

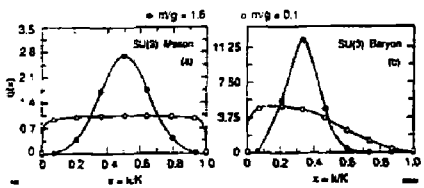

Figure 1. Valence structure functions of the baryon and meson in QCD in one-space and one-time dimension. The results are for one quark flavor and three colors.

The application of DLCQ to gauge theory in three-space and one-time dimensions is a much more challenging computational task, but progress has recently been made obtaining the spectrum of QED in the strong coupling domain.

In the following sections, I will discuss a number of general features of bound-state distributions for intrinsic gluons, bound-valence quarks, and intrinsic heavy-quark states. I will also discuss a new approach to shadowing and anti-shadowing in nuclear structure functions, which analytically relates these phenomena to quark and anti-quark nucleon scattering processes.

2. THE INTRINSIC GLUON DISTRIBUTION OF THE PROTON

The gluon distribution of a hadron is often assumed to be radiatively generated from QCD evolution of the quark structure functions beginning at an initial scale Q_0^2.[2] In such a model one assumes that there are no gluons in the hadron at a resolution scale below Q_0. The evolution is completely incoherent; i.e. each quark in the hadron radiates independently.

However, as can be seen in the light-cone Hamiltonian approach, the higher Fock components of a bound state in QCD contain gluons at any resolution scale. The exchange of gluon quanta in the bound state generates an interaction potential; the retardation (energy-dependent) part of the potential contributes to the intrinsic gluon distribution. Notice that the interference diagrams in which gluons are emitted from different quarks are not included in the usual extrinsic gluon distribution computed from the perturbative QCD evolution equations, since in leading twist these contributions only involve a single quark source.

More specifically, we can relate the distribution function of intrinsic photons in an atom or intrinsic gluons in a hadron to the hyperfine (spin-dependent) part of the bound state potential since both depend on the exchange of transverse gauge quanta. Each diagram that contributes to the transverse potential has a corresponding cut-diagram in the expression for the distribution function. In the actual calculation, these quantities differ by just a denominator D. Thus

$$\int_0^1 dx\, G_{g/B}\,(x,Q_0^2) \;=\; -\left\langle \frac{\partial V}{\partial M_B^2} \right\rangle_{Q_0^2} \quad ,$$

where $G_{g/B}$ is the unpolarized distribution function of gauge fields g in the bound state B, V is the potential due to gluon exchange and self-energy corrections, and

M_B is the bound-state mass. Note that the instantaneous (non-retarded) piece does not depend on M_B, so it does not contribute.

In the case of gluons in QCD bound states, we obtain:[3]

$$\int_0^1 dx \left[G_{g/p}(x) - G_{g/\Delta}(x) \right] = -\left\langle \frac{\Delta \partial V}{\partial M_B^2} \right\rangle_{kf_z} ,$$

for baryons (p and Δ).

The *intrinsic* gluon distribution $G_{g/H}(x, Q_0^2)$ describes the light-cone momentum distribution of gluons associated with the bound-state dynamics of the hadron H, in distinction to the *extrinsic* contributions which are derived from radiative processes or evolution. The intrinsic gluon distribution is derived from the solution of the non-perturbative bound state equation. In the case of quantum electrodynamics, one can readily calculate the photon distribution in positronium, to first order in the fine structure constant α. The analysis involves coherence between amplitudes in which the electron and positron couple to the photons. In the infrared limit this coherence in the neutral atom ensures a finite photon distribution.

In the QCD case, the analysis of the intrinsic gluon distribution of a hadron is essentially non-perturbative. However, there are several theoretical constraints which limit its form:

1. In order to insure positivity of fragmentation functions, distribution functions $G_{a/b}(x)$ must behave as an odd or even power of $(1-x)$ at $x \to 1$ according to the relative statistics of a and b.[4] Thus the gluon distribution of a nucleon must have the behavior: $G_{g/N}(x) \sim (1-x)^{2k}$ at $x \to 1$ to ensure correct crossing to the fragmentation function $D_{N/g}(x)$. This result holds individually for each helicity of the gluon and the nucleon.

2. The coupling of quarks to gluons tends to match the sign of the quark helicity to the gluon helicity in the large x limit.[5] We define the helicity-aligned and anti-aligned gluon distributions: $G^+(x) = G_{g\uparrow/N\uparrow}(x)$ and $G^-(x) = G_{g\uparrow/N\downarrow}(x)$. The gauge theory couplings imply

$$\lim_{x\to 1} G^-(x)/G^+(x) \to (1-x)^2.$$

3. In the low x domain, each of the quarks in the hadron radiate gluons coherently, and one must compute emission of gluons from the quark lines taking into account interference between amplitudes. Define $\Delta G(x) = G^+(x) - G^-(x)$ and $G(x) = G^+(x) + G^-(x)$. We find that the asymmetry ratio $\Delta G(x)/G(x)$ vanishes linearly with x; perhaps coincidentally, this is also the prediction from Reggeon exchange.[6] The coefficient at $x \to 0$ depends on the hadronic wavefunctions; however, for equal partition of the hadron's momentum among its constituents, we show that

$$\lim_{x\to 0} \Delta G(x)/G(x) \to N_q\, x,$$

where N_q is the number of valence quarks.

4. In the $x \to 1$ limit, the stuck quark is far off-shell so that one can use perturbation theory to characterize the threshold dependence of the structure functions. We find for three-quark bound states

$$\lim_{x\to 1} G^+(x) \to C(1-x)^{2N_q-2} = C(1-x)^4,$$

Thus $G^-(x) \to C(1-x)^6$ at $x \sim 1$. This is equivalent to the spectator-counting rule developed in Ref. 7.

We can write down a simple analytic model for the intrinsic gluon distribution in the nucleon which incor-

porates all of the above constraints:

$$\Delta G(x) = \frac{N}{x}[5(1-x)^4 - 4(1-x)^5 - (1-x)^6]$$

and

$$G(x) = \frac{N}{x}[5(1-x)^4 - 4(1-x)^5 + (1-x)^6]$$

In this model the momentum fraction carried by intrinsic gluons in the nucleon is $\langle x_g \rangle = \int_0^1 dx x G(x) = (10/21)N$, and the helicity carried by the intrinsic gluons is $\Delta G \equiv \int_0^1 dx \Delta G(x) = 7/6N$. The ratio $\Delta G / \langle x_g \rangle = 49/20$ for the intrinsic gluon distribution is independent of the normalization N. Phenomenological analyses imply that the gluons carry approximately one–half of the proton's momentum: $\langle x_{g/N} \rangle \simeq 0.5$. We shall assume that this is a good characterization of the intrinsic gluon distribution. The momentum sum rule then implies $N \sim 1$ and $\Delta G \sim 1.2$. In terms of anomalous contributions to the quark spin is concerned, this is a relatively small contribution. However, since $\frac{1}{2}\sum \Delta q + \Delta G + L_z = \frac{1}{2}$, a large fraction of the proton's angular momentum is associated with the gluon distribution. A review of the present experimental and theoretical limits on gluon and quark spin in the nucleon is given in Ref. 8.

The above equations give model forms for the polarized and unpolarized intrinsic gluon distributions in the nucleon which take into account coherence at low x and perturbative constraints at high x. It is expected that this should be a good characterization of the gluon distribution at the resolution scale $Q_0^2 \simeq M_p^2$.

It is well–known that the leading power at $x \sim 1$ is increased when QCD evolution is taken into account. The change in power is

$$\Delta p_g(Q^2) = 4C_A\, \zeta(Q^2, Q_0^2) = \frac{1}{\pi}\int_{Q_0^2}^{Q^2} \frac{d\kappa^2}{\kappa^2}\alpha_s(\kappa^2),$$

where $C_A = 3$ in QCD. For typical values of $Q_0 \sim 1\ GeV$, $\Lambda_{\overline{MS}} \sim 0.2\ GeV$ the change in power is moderate: $\Delta p_g(2\ GeV^2) = 0.28$, $\Delta p_g(10\ GeV^2) = 0.78$. A recent determination of the unpolarized gluon distribution of the proton at $Q^2 = 2\ GeV^2$ using direct photon and deep inelastic data has been given in Ref. 9. The best fit over the interval $0.05 \le x \le 0.75$ assuming the form $xG(x, Q^2 = 2\ GeV^2) = A(1-x)^{\eta_g}$ gives $\eta_g = 3.9 \pm 0.11(+0.8 - 0.6)$, where the errors in parenthesis allow for systematic uncertainties. This result is compatible with the prediction $\eta_g = 4$ for the intrinsic gluon distribution at the bound–state scale, allowing for the increase in the power due to evolution. HERA experiments could provide a definitive check on the shape and large–x behavior of the gluon structure function.

3. BOUND VALENCE–QUARK DISTRIBUTIONS

An important concept in the description of any bound state is the definition of "valence" constituents. In atomic physics the term "valence electrons" refers to the electrons beyond the closed shells which give an atom its chemical properties. Correspondingly, the term "valence quarks" refers to the quarks which give the bound state hadron its global quantum numbers. In quantum field theory, the valence quarks appear in each Fock state together with any number of gluons and quark–anti–quark pairs; each component thus has the global quantum numbers of the hadron.

How can one identify the contribution of the valence quarks of the bound state with the phenomenological structure functions? Traditionally, the distribution function $G_{q/H}$ has been separated into "valence" and "sea" contributions:[10] $G_{q/H} = G^{\rm val}_{q/H} + G^{\rm sea}_{q/H}$, where, as an operational definition, one assumes

$$G^{\rm sea}_{q/H}(x, Q^2) = G^{\rm sea}_{\overline{q}/H}(x, Q^2), \qquad (0 < x < 1),$$

and thus $G^{\rm val}_{q/H}(x, Q^2) = G_{q/H}(x, Q^2) - G_{\overline{q}/H}(x, Q^2)$. The assumption of identical quark and anti–quark sea distributions is plausible for the s and $\overline{s}$ quarks in the

proton. However, in the case of the u and d quark contributions to the sea, anti-symmetrization of identical quarks in the higher Fock states implies non-identical q and $\bar{q}$ sea contributions. This is immediately apparent in the case of atomic physics, where Bethe-Heitler pair production in the field of an atom does not give symmetric electron and positron distributions since electron capture is blocked in states where an atomic electron is already present. Similarly, in QCD, the $q\bar{q}$ pairs which arise from gluon splitting do not have identical quark and anti-quark sea distributions; contributions from interference diagrams, which arise from the anti-symmetrization of the higher Fock state wavefunctions, must be taken into account. Notice that because of wave-function normalization, the exclusion principle does not affect the value of conserved charges such as $\int_0^1 dx(G_{q/B}(x) - G_{\bar{q}/B}(x))$. Thus even though the conventional separation of valence and sea contributions gives correct charge sum rules, it can give a misleading reading of the actual momentum distribution of the valence quarks.

The standard definition also has the difficulty that the derived valence quark distributions are apparently singular in the limit $x \to 0$. For example, standard phenomenology indicates that the valence up-quark distribution in the proton behaves as $G^{val}_{u/p} \sim x^{-\alpha_R}$ for small x[10,11] where $\alpha_R \approx 0.5$. Note that the position α_R of J-plane singularities in the forward virtual Compton amplitude are Q^2-independent, and thus the non-singlet Reggeon behavior $F_2^{NS}(x,Q^2) \sim x^{1-\alpha_R}$ at $x \to 0$ must be unaffected by QCD evolution.[12] This implies that quantities that depend on the $(1/x)$ moment of the valence distribution diverge. This is the case for the "sigma term" in current algebra and the $J = 0$ fixed pole in Compton scattering.[13] Furthermore, it has been shown[14] that the change in mass of the proton when the quark mass is varied in the light-cone Hamiltonian is given by an extension of the Feynman-Hellmann theorem:

$$\frac{\partial M_p^2}{\partial m_q^2\,(Q^2)} = \int_0^1 \frac{dx}{x}\, G_{q/p}\,(x,Q^2).$$

In principle, this formula allows one to compute the contribution to the proton-neutron mass difference due to the up and down quark masses. However, again, with the standard definition of the valence quark distribution, the integration is undefined at low x. Even more seriously, the expectation value of the light-cone kinetic energy operator

$$\int_0^1 dx\, \frac{\langle k_\perp^2 \rangle + m^2}{x}\, G_{q/p}(x,Q).$$

is infinite for valence quarks if one uses the traditional definition. There is no apparent way of associating this divergence of the kinetic energy operator with renormalization.

Part of the difficulty with identifying bound state contributions to the proton structure functions is that many physical processes contribute to the deep inelastic lepton-proton cross section: From the perspective of the laboratory or center of mass frame, the virtual photon can scatter out a bound-state quark as in the atomic physics photoelectric process, or the photon can first make a $q\bar{q}$ pair, either of which can interact in the target. As we emphasize here, in such pair-production processes, one must take into account the Pauli principle which forbids creation of a quark in the same state as one already present in the bound state wavefunction. Thus the lepton interacts with quarks which are both *intrinsic* to the proton's bound-state structure, and with quarks which are *extrinsic*; i.e. created in the electron-proton collision itself. Notice that such extrinsic processes would occur in electroproduction even if the valence quarks had no charge. Thus much of the phenomena observed in electroproduction at small values of

x, such as Regge behavior, sea distributions associated with photon–gluon fusion processes, and shadowing in nuclear structure functions should be identified with the extrinsic interactions, rather than processes directly connected with the proton's bound-state structure.

Recently, Schmidt and I[15] have proposed a new definition of "bound valence-quark" distribution functions that correctly isolates the contribution of the valence constituents which give the hadron its flavor and other global quantum numbers. With this new separation, $G_{q/p}(x,Q^2) = G^{\rm BV}_{q/p}(x,Q^2) + G^{\rm NV}_{q/p}(x,Q^2)$, the non-valence quark distributions are identified with the structure functions which would be measured if the valence quarks of the target hadron had zero electro-weak charge. We can show that with this new definition the bound valence-quark distributions $G^{\rm BV}_{q/p}(x,Q^2)$ vanish at $x \to 0$, as expected from the wave function of a bound-state constituent.

In order to construct the bound valence-quark distributions, we imagine a *gedanken* QCD where, in addition to the usual set of quarks $\{q\} = \{u,d,s,c,b,t\}$, there is another set $\{q_0\} = \{u_0,d_0,s_0,c_0,b_0,t_0\}$ with the same spin, masses, flavor, color, and other quantum numbers, except that their electromagnetic charges are zero. Let us now consider replacing the target proton p in the lepton-proton scattering experiment by a charge-less proton p_0 which has valence quarks q_0 of zero electromagnetic charge. In this extended QCD of the higher Fock wavefunctions of the proton p and the charge-less proton p_0 both contain $q\bar{q}$ and $q_0\bar{q}_0$ pairs. As far as the strong QCD interactions are concerned, the physical proton and the *gedanken* charge-less proton are equivalent.

We then define the bound valence-structure function of the proton from the difference between scattering on the physical proton minus the scattering on the charge-less proton, in analogy to an "empty target" subtraction:

$$F_i^{\rm BV}(x,Q^2) \equiv F_i^{p}(x,Q^2) - F_i^{p_0}(x,Q^2).$$

The non-valence distribution is thus $F_i^{\rm NV}(x,Q^2) = F_i^{p_0}(x,Q^2)$. Here the $F_i(x,Q^2)$ ($i = 1,2$, etc.) are the leading twist structure functions. The situation just described is similar to the atomic physics case, where in order to correctly define photon scattering from a bound electron, one must subtract the cross section on the nucleus alone, without that bound electron present.[16] Physically, the nucleus can scatter photons through virtual pair production, and this contribution has to be subtracted from the total cross section. In QCD we cannot construct protons without the valence quarks; thus we need to consider hadrons with charge-less valence constituents.

In order to specifically isolate the bound valence d-quark distribution of the proton $p(uud)$, we subtract the deep inelastic cross section on the system $p_0(uud_0)$ in which the d_0 valence quark has normal QCD interactions but does not carry electric charge. (Both p and p_0 contain higher Fock states with arbitrary number of gluons, $q\bar{q}$, and $q_0\bar{q}_0$ pairs.) It is clear that the terms associated with $J \approx 1$ Pomeron behavior due to gluon exchange cancel in the difference. We also can show that the Reggeon terms also cancel, and thus the resulting distribution of bound valence d quarks $G^{\rm BV}_{d/p}(x,Q^2) = \left[[F_2^{p(uud)}(x,Q^2) - F_2^{p_0(uud_0)}(x,Q^2)]/e_d^2\, x\right]$ vanishes as $x \to 0$.

The high Q^2 virtual photo-absorption cross section on the proton (lab frame) contains two types of terms: contributions in which a quark in p absorbs the momentum of the virtual photon; and terms in which a $q\bar{q}$ pair is created, but the produced q is in a different quantum state than the quarks already present in the hadron. On the other hand, the cross section for scattering of the virtual photon from the state $p_0(uud_0)$ contains contributions that differ from the $p(uud)$ case in two important aspects: first the virtual photon can be absorbed only by charged quarks; and in $d\bar{d}$ pair production on the null proton p_0, the d quark can be produced in any

state. Thus the difference between the cross sections off p and p_0 equals a term (analogous to $\sigma_{\text{photoelectric}}$ in atomic physics), in which a d quark in p absorbs the photon momentum, minus a $d\bar{d}$ pair production contribution on p_0 (analogous to a capture cross section in atomic physics), in which the produced $\bar{d}$ quark ends up in the same quantum state as the d quark in the original proton state p.[17] This is shown graphically in Fig. 2.

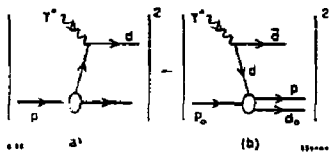

Figure 2. The bound valence-quark distribution of quark d is calculated from the difference between (a) the cross section on the state $p(uud)$ in which the virtual photon momentum is absorbed by the quark d, and (b) the $d\bar{d}$ pair production cross section in the field of the gedanken baryon $p_0(uud_0)$, where the produced $\bar{d}$ quark is captured in the same state as the d quark in the original proton state p.

Reggeon behavior in the electroproduction cross section can be understood as due to the appearance of a spectrum of bound $q\bar{q}$ states in the t−channel. The summation of such diagrams leads to Reggeon behavior of the deep inelastic structure functions at small x.[18] In the rest system, the virtual photon creates a $d\bar{d}$ pair at a distance proportional to $1/x$ before the target. The radiation which occurs over this distance contributes to the physics of the Reggeon behavior. In the case of the proton target, the d−quark, after radiation, cannot appear in the quantum state already occupied by the d−quark in the proton because of the Pauli principle. However, the corresponding contribution is allowed on the p_0 target: in effect, the d−quark replaces the d_0−quark and is captured into a proton. The capture cross section is computed from the amplitude for $\gamma^* p_0 \to \bar{d}^* p\, d_0$.[19] As in the corresponding atomic physics analysis, the spectator d_0 quark in the null target p_0 is inert and cancels out from the amplitude. Thus we only need to consider effectively the (helicity summed) squared amplitude for $\gamma^*(uu) \to \bar{d}^* p$. However, as illustrated in Fig. 3 this amplitude, after charge conjugation and crossing $s \to u$, is equal to the (helicity summed) $\gamma^* p \to d^*(uu)$ amplitude at small x. The flux factors for the proton and null proton target are equal.

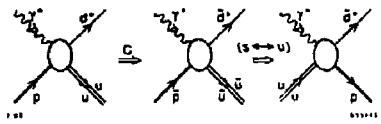

Figure 3. The helicity-summed squared amplitude for (a) $\gamma^* p \to d(uu)$ is equal, by charge conjugation, to the helicity-summed squared amplitude for the process (b) $\gamma^* \bar{p} \to \bar{d}(\bar{u}\bar{u})$, up to a phase. This is also equal, by crossing symmetry, to the helicity-summed squared amplitude for (c) $\gamma^*(uu) \to \bar{d}p$, with s and u interchanged.

If we write $s\sigma_{\text{photoelectric}}$ as a sum of Regge terms of the form $\beta_R |s|^{\alpha_R}$, where $\alpha_R > 0$ then the subtraction of the capture cross section on the null proton will give the net virtual photo-absorption cross section as a sum of terms $s\sigma^{\text{BV}} = \sum_R \beta_R (|s|^{\alpha_R} - |u|^{\alpha_R})$. If we ignore mass corrections in leading twist, then $s \simeq Q^2(1-x)/x$ and $u \simeq -Q^2/x$. Thus for small x every Regge term is multiplied by a factor $K_R = (-\alpha_R)x$. For example, for $\alpha_R \approx 1/2$ (which is the leading even charge-conjugation Reggeon contribution for non-singlet isospin structure functions). $F_2^{p(uud)} - F_2^{p_0(uud_0)} \sim x^{3/2}$. The bound valence-quark non-singlet ($I = 1$) distribution thus has leading behavior $G^{\text{BV}}_{q/H} \sim x^{1/2}$ and vanishes for $x \to 0$.

We can also understand this result from symmetry considerations. We have shown from crossing symmetry $G_{q/p}(x, Q^2) - G_{\bar{q}/p_0}(x, Q^2) = 0$ at low x. Thus the even charge-conjugation Reggeon and Pomeron contributions decouple from the bound valence-quark distributions.

The essential reason why the new definition of the bound valence-quark distribution differs from the conventional definition of valence distributions is the Pauli

principle: the anti-symmetrization of the bound state wavefunction for states which contain quarks of identical flavor. As we have shown, this effect plays a dynamical role at low x, eliminating leading Regge behavior in the bound valence-quark distributions. In the atomic physics case, where there is no leading Regge behavior, the analogous application of the Pauli principle leads to analytic consistency with the Kramers-Kronig dispersion relation for Compton scattering on a bound electron.[16]

4. INTRINSIC CHARM-QUARK DISTRIBUTIONS

There are a number of striking anomalies in the data[20] for charm production which cannot be readily explained by conventional fusion subprocesses.

1. The EMC data[21] for the charm structure function of the nucleon appears to be too high at large x_{Bj}.
2. The LEBC bubble chamber data[22] for charm production in pp collisions indicates an excess of D events at large X_F. The excess is not associated with $D's$ that contain the proton's valence quark.
3. The cross section measured by the WA-62 group[23] for $\Sigma^- N \to \Xi(csu)X$ is too large and flat at large X_F.
4. The NA-3 data[24] for J/ψ production in pion-nucleus and proton-nucleus collisions can be represented as two components: a normal contribution in the central region which is almost additive in nuclear number that can be accounted for by $gg \to c\bar{c}$ and $q\bar{q} \to c\bar{c}$ fusion, and a second "diffractive contribution" which dominates at large x_F and is strongly shadowed. This last contribution indicates that high momentum $c\bar{c}$ systems are being produced on the surface of the nuclear target.

It is difficult to understand any of these anomolies, particularly the production of high x_F charmonium unless the proton itself has an intrinsic charm contribution[25] to its structure function. If these charm quarks are associated with the bound-state equation for the proton, then all the partons tend to have equal velocity. This implies that the heaviest constituents, the intrinsic charm quarks, will take a large fraction of the proton's momentum. In a hadronic collision the c and $\bar{c}$ can coalesce to produce a charmonium state with the majority of the proton's momentum.[26] The EMC charm structure function data requires a 0.3 % probability for the intrinsic charm Fock state in the nucleon.[21]

According to the hard scattering picture of QCD, production cross sections involving large momentum transfer should factorize and be approximately additive in the nucleon number, $d\sigma_A = A^\alpha(x_F, p_T) d\sigma_N$ with $\alpha \sim 1$, up to the small shadowing and anti-shadowing corrections seen in deep inelastic lepton-nucleus scattering. I will return to these effects in the next section.

In the Drell-Yan process, large mass muon pair production, $\alpha \simeq 1$ for all x_F is indeed observed.[30] However, several experiments on open charm production show[20] that $\alpha(x_F \geq 0.2) \simeq 0.7 \ldots 0.8$. For small x_F, an indirect analysis[22] comparing different measurements of the total charm production cross section indicates $\alpha(x_F \simeq 0) \simeq 1$. More detailed data on the nuclear dependence of charm production is available from the hadroproduction of J/ψ. Here a decrease of α from $\alpha(x_F \simeq 0) \simeq 1$ to $\alpha(x_F \simeq 0.8) \simeq 0.8$ has been seen by several groups.[31] The analysis of Badier, *et al.*[24] is particularly interesting. They noted that the production of J/ψ at large x_F (up to $x_F \simeq 0.8$) cannot be explained by the gluon and light quark fusion mechanisms of perturbative QCD, due to the anomalous A-dependence. However, their $\pi^- A \to J/\psi + X$ data was well reproduced if, in addition to hard QCD fusion (with $\alpha = 0.97$), they included a "diffractive" component of J/ψ production at high x_F with $\alpha = 0.77$. Using their measured A-dependence to extract the "diffractive" component, they found that

(for a pion beam) that the J/ψ distribution peaks at $x_F \simeq 0.5$ and dominates the hard scattering A^1 component for $x \gtrsim 0.6$.

A diffractive contribution to heavy quarkonium production is consistent with QCD. In high energy hadron-nucleus collisions the nucleus may be regarded as a "filter" of the hadronic wave function.[28] The argument, which relies only on general features such as time dilation, goes as follows.[27] Consider the equal-time Fock state expansion of a hadron in terms of its quark and gluon constituents; *e.g.*, for a meson,

$$|h\rangle = |q\bar{q}\rangle + |q\bar{q}g\rangle + |q\bar{q}q\bar{q}\rangle + \cdots$$

The various Fock components will mix with each other during their time evolution. However, at sufficiently high hadron energies E_h, and during short times t, the mixing is negligible. Specifically, the relative phase $\exp[-i(E - E_h)t]$ of a given term in Eq. (1) is proportional to the energy difference

$$E - E_h = \left[\sum_i \frac{m_i^2 + p_{Ti}^2}{x_i} - M_h^2\right] \Big/ (2E_h)$$

which vanishes for $E_h \to \infty$. Hence the time evolution of the Fock expansion is, at high energies, diagonal during the time $\sim 1/R$ it takes for the hadron to cross a nucleus of radius R.

The diagonal time development means that it is possible to describe the scattering of a hadron in a nucleus in terms of the scattering of its individual Fock components. Let us explore the consequences for typical, soft collisions characterized by momentum transfers $q_T \simeq \Lambda_{QCD}$. The partons of a given Fock state will scatter independently of each other if their transverse separation is $r_T \gtrsim 1/\Lambda_{QCD}$; *i.e.* if the state is of typical hadronic size. Conversely, the nuclear scattering will be coherent over the partons in Fock states having $r_T \ll 1/\Lambda_{QCD}$ since $e^{iq_T \cdot r_T} \simeq 1$. For color-singlet clusters, the interference between the different parton amplitudes interacting with the nuclear gluonic field is destructive. Thus the nucleus will appear nearly transparent to small, color-singlet Fock states.[29] In an experiment detecting fast secondary hadrons the nucleus indeed serves, then, as a filter that selects the small Fock components in the incident hadrons.

Consider the intrinsic charm state $|u\bar{d}c\bar{c}\rangle$ of a $|\pi^+\rangle$. Because of the large charm mass m_c, the energy difference in denominator of the wavefunction will be minimized when the charm quarks have large x, *i.e.* when they carry most of the longitudinal momentum. Moreover, because m_c is large, the transverse momenta p_{Tc} of the charm quarks range up to $\mathcal{O}(m_c)$, implying that the transverse size of the $c\bar{c}$ system is $\mathcal{O}(1/m_c)$. Hence, provided only that the $c\bar{c}$ forms a color singlet, it can penetrate the nucleus with little energy loss. Thus the high momentum small transverse size $c\bar{c}$ color-singlet cluster in the incident hadron passes through the nucleus undeflected, and it can then evolve into charmonium states after transiting the nucleus.[32] In effect, the nucleus is transparent to the heavy quark pair component of the intrinsic state. The remaining cluster of light quarks in the intrinsic charm Fock state is typically of hadronic size and will interact strongly on the front surface of the nucleus. Consequently, the A-dependence of the cross section is given by the geometrical factor, $\alpha \simeq 2/3$. This justifies the analysis of Badier *et al.*[24] in which the perturbative and non-perturbative charm production mechanisms were separated on the basis of their different A-dependence ($\alpha = 0.97$ and $\alpha = 0.77$ for a pion beam, respectively). The effective x_F-dependence of α seen in charm production is explained by the different characteristics of the two production mechanisms. Hard, gluon fusion production dominates at small x_F, due to the steeply falling gluon structure function. The contribution from intrinsic charm Fock states in the beam peaks at higher x_F, due to the large momentum carried by

the charm quarks. This two-component hard-scattering plus intrinsic charm model also explains why the nuclear dependence of J/ψ production depends on x_F rather than x_2, as predicted by leading twist factorization.[33]

An important consequence of this picture is that all final states produced by a penetrating intrinsic $c\bar{c}$ component will have the same A-dependence. Thus, in particular, the $\psi(2S)$ radially excited state will behave in the same way as the J/ψ, in spite of its larger size. The nucleus cannot influence the quark hadronization which (at high energies) takes place outside the nuclear environment.

Quarkonium production due to the intrinsic heavy quark state will fall off rapidly for p_T greater than M_Q, reflecting the fast-falling transverse momentum dependence of the higher Fock state wavefunction. Thus we expect the conventional fusion contributions to dominate in the large p_T region. The data are in fact consistent with a simple A^1 law for J/ψ production at large p_T. The CERN experiment of Badier *et al.*[24] finds that the ratio of nuclear cross sections is close to additive in A for all x_F when p_T is between 2 and 3 GeV. The data of the FermiLab experiment of Katsanevas *et al.*[31] shows consistency with additivity for p_T ranging from 1.2 to 3 GeV.

The probability for intrinsic heavy quark states in a light hadron wave function is expected[25,34] to scale with the heavy quark mass M_Q as $1/M_Q^2$. This implies a production cross section proportional to $1/M_Q^4$. The total rate of heavy quark production by the intrinsic mechanism therefore decreases with quark mass, compared to the perturbative cross section which is proportional to $1/M_Q^2$. At large x the intrinsic production should still dominate, however, implying a nuclear dependence in this region characterized by $\alpha \simeq 0.7 \ldots 0.8$. Experimental measurements of beauty hadroproduction in nuclei over the whole range of x will be essential for unraveling the two components of the cross section.

5. SHADOWING AND ANTI-SHADOWING OF NUCLEAR STRUCTURE FUNCTIONS

The shadowing and anti-shadowing of deep inelastic nuclear structure functions refers to the depletion of the effective number of nucleons F_2^A/F_2^N at low $x \lesssim 0.1$, and the increase above nucleon additivity at $x \sim 0.15$. Results from the EMC collaboration[35] and SLAC[36] indicate that the effect is roughly Q^2-independent; *i.e.* shadowing is a leading twist in the operator product analysis In contrast, the shadowing of the real photo-absorption cross section due to ρ-dominance[37-40] falls away as an inverse power of Q^2.

Shadowing is a destructive interference effect which causes a diminished flux and interactions in the interior and back face of the nucleus. The Glauber analysis[41] corresponds of hadron-nucleus scattering to the following: the incident hadron scatters elastically on a nucleon N_1 on the front face of the nucleus. At high energies the phase of the amplitude is imaginary. The hadron then propagates through the nucleus to nucleon N_2 where it interacts inelastically. The accumulated phase of the hadron propagator is also imaginary, so that this two-step amplitude is coherent and opposite in phase to the one-step amplitude where the beam hadron interacts directly on N_2 without initial-state interactions. Thus the target nucleon N_2 sees less incoming flux: it is shadowed by elastic interartions on the front face of the nucleus. If the hadron-nucleon cross section is large, then for large A the effective number of nucleons participating in the inelastic interactions is reduced to $\sim A^{2/3}$, the number of surface nucleons.

In the case of virtual photo-absorption, the photon converts to a $q\bar{q}$ pair at a distance before the target proportional to $\omega = x^{-1} = 2p \cdot q/Q^2$ in the laboratory frame.[42] In a physical gauge, such as the light-

cone $A^+ = 0$ gauge, the final-state interactions of the quark can be neglected in the Bjorken limit, and effectively only the anti-quark interacts. The nuclear structure function F_2^A producing quark q can then be written as an integral[43,44] over the inelastic cross section $\sigma_{\bar{q}A}(s')$ where s' grows as $1/x$ for fixed space-like anti-quark mass. Thus the A-dependence of the cross section mimics the A-dependence of the $\bar{q}$ cross section in the nucleus. Hung Jung Lu and I have recently applied the standard Glauber multi-scattering theory, to $\sigma_{\bar{q}A}$ assuming that formalism can be taken over to off-shell $\bar{q}$ interactions.[45] The shadowing mechanism is illustrated in Fig. 4.

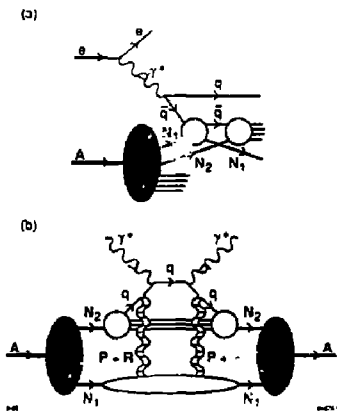

Figure 4. (a) The double-scattering amplitude that shadows the direct interaction of the anti-quark with N_2. (b) The same mechanism as in (a), drawn in the traditional "hand-bag" form. Pomeron and Reggeon exchange between the quark line and N_1 are explicitly illustrated.

Our results show that for reasonable values of the $\bar{q}$-nucleon cross section, one can understand the magnitude of the shadowing effect at small x. Moreover, if one introduces an $\alpha_R \simeq 1/2$ Reggeon contribution to the $\bar{q}N$ amplitude, the real phase introduced by such a contribution automatically leads to "anti-shadowing" (effective number of nucleons $F_2^A(x,Q^2)/F_2^N(x,Q^2) > A$) at $x \simeq 0.15$ of the few percent magnitude seen by the SLAC and EMC experiments.[35,36]

Our analysis provides the input or starting point for the log Q^2 evolution of the deep inelastic structure functions, as given for example by Mueller and Qiu.[46] The parameters for the effective $\bar{q}$ nucleon cross section required to understand shadowing phenomena provide important information on the interactions of quarks in nuclear matter. This analysis also has implications of the nature of particle production for virtual photoabsorption in nuclei. At high Q^2 and $x > 0.3$, hadron production should be uniform throughout the nucleus. At low x where shadowing occurs, the inelastic reaction occurs mainly at the front surface. These features can be examined in detail by studying non-additive multiparticle correlations in both the target and current fragmentation region. It should also be emphasized that the same types of multi-scattering "fan" diagrams also appear in the analysis of the saturation of the gluon distribution at small x.[47]

The results for the effective number of nucleons $A_{eff}(x)/A$ are shown in Fig. 5 for $A = 12$, 64, and 238. One observes shadowing below $x \simeq 0.1$ and an anti-shadowing peak around $x \simeq 0.15$. The shadowing effects are roughly logarithmic on the mass number A. The magnitude of shadowing predicted by the model is consistent with the data for $x > 0.01$; below this region, one expects higher-twist and vector-meson dominance shadowing to contribute. For $x > 0.2$ other nuclear effects must be taken into account. Most of the parameters used in the model are assigned typical hadronic values. The critical quantity is the effective quark-nucleon cross section σ which controls the magnitude of shadowing effect near $x = 0$: a larger value of σ implies a larger $\bar{q}^4N$ cross section and thus more shadowing. Notice that σ is the effective cross section at zero $\bar{q}$ virtuality, thus the typical value $\langle\sigma\rangle$ entering the calculation is somewhat smaller. The magnitude of anti-shadowing

is determined the real to imaginary-part ratio of the Reggeon scattering amplitude.

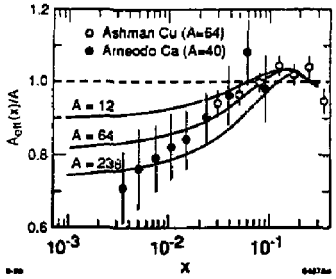

Figure 5 The predicted ratio of $A_{eff}(x)/A$ of the multi-scattering model in the low x region for different nuclear mass number. The data points are results from the EMC experiment for Cu and Ca.

Our semi-quantitative analysis shows that parton multiple-scattering process provides a mechanism for explaining the observed shadowing at low x in the EMC-SLAC data. The existence of anti-shadowing requires the presence of regions where the real part of the $\overline{q} - N$ amplitude dominates over the imaginary part. The constructive interference which gives anti-shadowing in the $x \sim 0.15$ region is due in this model to the phase of the Reggeon $\alpha = 1/2$ term. The phase follows from analyticity and is dictated by the shape of the structure functions at low x. We could utilize additional terms (at lower values of α) to parameterize other bound-state contributions which vanish as higher powers of x, but in practice their qualitative effect would be indistinguishable from the our simplified model.

The analysis presented here correlates shadowing phenomena to microscopic quark-nucleon parameters. This approach also provides a dynamical and analytic explanation of anti-shadowing, confirming the conjecture of Nikolaev and Zakharov[48] who predicted that such an effect must exist on the basis of conservation laws. Using the perturbative QCD factorization theorem for inclusive reactions, the same analysis can be extended to Drell-Yan and other fusion processes, taking into account the separate dependence on the valence and sea quarks. Thus some shadowing and anti-shadowing should also be observable in the nuclear structure function $F_2^A(x_2, Q^2)$ extracted from massive lepton pair production on nuclear targets at low x_2.

6. TESTS AT HERA

Many of the topics I have discussed in this talk can be directly tested at HERA.

1. The QCD model for intrinsic gluons presented in section 2, evolved to HERA momentum transfers, provides detailed predictions for the small x and large x behavior of the gluon and sea quark distributions.

2. Measurements of non-singlet structure functions in charged current reactions and the difference of proton and neutron cross sections using a deuteron beam at HERA will be very important for confirming non-singlet Regge behavior of the leading twist structure functions. This will allow the construction of the Regge-free bound-valence quark distributions discussed in section 3.

3. Studies of shadowing and anti-shadowing processes on nuclei would be very interesting at HERA energies. Some information can be obtained with deuteron beams, but the possibility of heavy ion beams should be explored.

4. Diffractive reactions where the proton is tagged in the forward direction lead to fundamental probes of the Pomeron and will give more insight into the multi-gluon matrix elements needed to understand saturation of the gluon structure function.[49] Diffraction of light mass vector meson systems is also important for understanding high energy exclusive reactions and shadowing mecha-

nisms. Electroproduction of the π^0 at high energies would be an ideal way to isolate the Odderon in the t-channel, the odd charge conjugation counterpart of the Pomeron predicted by QCD.

5. HERA is the ideal laboratory to confirm or disprove the presence of intrinsic charm and beauty in the proton. Intrinsic heavy quark states can be identified two ways: by flavor-tagging the recoil jet and spectator system in the proton beam direction; and by measuring the longitudinal momentum distribution of heavy quarkonium in the proton fragmentation region in electron-proton collisions. The presence of charm and beauty in the nucleon at large x would have important implications for our fundamental understanding of hadrons in QCD.

ACKNOWLEDGEMENTS

The work reported here was based on collaborations with Kent Hornbostel, Paul Hoyer, Hung Jung Lu, Al Mueller, Chris Pauli, and Ivan Schmidt. This work was supported by the Department of Energy, contract DE-AC03-76SF00515.

REFERENCES

1. K. Hornbostel, S. J. Brodsky, and H.-C. Pauli, Phys. Rev. D41, 3814 (1990); K. Hornbostel, SLAC-0333, Ph. D. thesis, unpublished (1988); and M. Burkardt, Nucl. Phys. A504, 762 (1989); and references therein.
2. See, e. g., F. Martin, Phys. Rev. D19, 1382 (1979); M. Glück, E. Reya, and W. Vogelsang, Dortmund University preprint DO-TH-89/3 (1989).
3. S. J. Brodsky and I.A. Schmidt, Phys. Lett. B234, 144 (1990.)
4. V. N. Gribov and L. N. Lipatov, Sov. J. Nucl. Phys. 15, 438 and 675 (1972).
5. J. D. Bjorken, Phys. Rev. D1, 1376 (1970).
6. See, for example, S. J. Brodsky, J. Ellis, M. Karliner, Phys. Lett. B206, 309 (1988).
7. R. Blankenbecler, S. J. Brodsky Phys. Rev. D10, 2973 (1974); J. F. Gunion, Phys. Rev. D10, 242 (1974); S. J. Brodsky and J. F. Gunion, Phys. Rev. D19, 1005 (1979), where coherence effects are also discussed.
8. M. Karliner, 24th Rencontre de Moriond, Mar 1989; preprint TAUP 1730-89.
9. P. Aurenche, *et al.*, Phys. Rev. D39, 3275 (1989).
10. See, for example, F. E. Close, *An Introduction to Quarks and Partons*, Academic Press (1979).
11. J. Kuti and V. F. Weisskopf, Phys. Rev. D4, 3418 (1971).
12. We thank J. Collins for conversations on this point.
13. S. J. Brodsky, F. E. Close and J. F. Gunion, Phys. Rev. D5, 1384 (1972).
14. W. Weisberger, Phys. Rev. D5, 2600 (1972); S. J. Brodsky, F. E. Close and J. F. Gunion, Phys. Rev. D8, 3678 (1973); S. J. Brodsky and I. Schmidt, unpublished. This result assumes that the valence quark mass only appears in the light-cone kinetic energy $\sum(k_\perp^2 + m^2)/x$.
15. S. J. Brodsky and I. A. Schmidt, SLAC-PUB-5169 (1990).
16. M. L. Goldberger and F. E. Low, Phys. Rev. 176, 1778 (1968); see also: T. Erber, Ann. Phys. 6, 319 (1959).
17. We neglect processes higher order in α_{QED} such as pair production in the electromagnetic field of the quark d.

18. For a derivation of the Reggeon contribution to the leading twist structure functions, see P. V. Landshoff, J. C. Polkinghorne and R. Short, Nucl. Phys. B28, 224 (1971), and S. J. Brodsky, F. E. Close, and J. F. Gunion, Phys. Rev. D8, 3678 (1973).

19. As usual we neglect hadronization effects and other final state interactions at high energies.

20. S. P. K. Tavernier, Rep. Prog. Phys. 50, 1439 (1987); U. Gasparini, Proc. XXIV Int. Conf. on High Energy Physics, (R. Kotthaus and J. H. Kühn, Eds., Springer 1989), p. 971.

21. Detailed predictions for the contribution of intrinsic charm to the nucleon charmed quark structure functions and comparisons with existing leptoproduction data are given by E. Hoffmann and R. Moore Z. Phys. C20, 71 (1983).

22. M. MacDermott and S. Reucroft, Phys. Lett. 184B, 108 (1987).

23. S. F. Biagi, *et al.*, Z. Phys. C28, 175 (1985). See also P. Coteus, *et al.*, Phys. Rev. Lett. 59, 5030 (1987).

24. J. Badier, *et al.*, Z. Phys. C20, 101 (1983); J. Badier, *et al.*, Phys. Lett. 104B, 335 (1981).

25. S. J. Brodsky, P. Hoyer, C. Peterson, and N. Sakai, Phys. Lett. 93B, 451 (1980); S. J. Brodsky, C. Peterson, and N. Sakai, Phys. Rev. D23, 2745 (1981).

26. S. J. Brodsky, J. F. Gunion, and D. E. Soper, Phys. Rev. D36, 2710 (1987).

27. S. J. Brodsky, P. Hoyer Phys. Rev. Lett. 63, 1566 (1989).

28. G. Bertsch, S. J. Brodsky, A. S. Goldhaber, and J. F. Gunion, Phys. Rev. Lett. 47, 297 (1981). In this paper the "color filter" argument was used to predict the production in nuclei of diffractive high mass multi-jet final states with momentum distributions controlled by the structure of the valence Fock state of the incident hadrons.

29. The diminished interactions of small color-singlet Fock components also leads to the phenomena of "color transparency" in quasi-elastic hadron-nucleon scattering inside of nuclei. See A. H. Mueller, Proc. XVII Recontre de Moriond (1982), and S. J. Brodsky, Proc. XIII Int. Symp. on Multiparticle Dynamics, Volendam (1982). In this case the dominance of small valence Fock components in large momentum transfer exclusive reactions implies the absence of initial and final state interactions. Experimental evidence for color transparency in quasi elastic pp scattering in nuclei at beam momentum up to 10 GeV/c is given in A. S. Carroll, et. al, Phys. Rev. Lett. 61, 1698 (1988). Explanations for the absence of color transparency at 12 GeV/c are given in S. J. Brodsky, G. F. De Teramond, Phys. Rev. Lett. 60, 1924 (1988); and in J. P. Ralston and B. Pire, Phys. Rev. Lett. 61, 1823 (1988).

30. K. J. Anderson, *et al.*, Phys. Rev. Lett. 42, 944 (1979); A. S. Ito, *et al.*, Phys. Rev. D23, 604 (1981); P. Bordalo, *et al.*, Phys. Lett. 193B, 368 (1987).

31. Yu. M. Antipov, *et al.*, Phys. Lett. 76B, 235 (1978); M. J. Corden, *et al.*, Phys. Lett. 110B, 415 (1982); J. Badier, *et al.*, Z. Phys. C20, 101 (1983); S. Katsanevas, *et al.*, Phys. Rev. Lett. 60, 2121 (1988).

32. Alternatively, the individual charmed quarks can fragment into final state charmed hadrons either by hadronization or by coalescing with co-moving light quark spectators from the beam. This effect can explain the depletion of the ratio of J/ψ to continuum muon pairs in high transverse energy

nucleus-nucleus collisions. See S J. Brodsky and A. H. Mueller, Phys. Lett. B206, 685 (1988).

33. P. Hoyer, M. Vanttinen, and U. Sukhatme, HU-TFT-90-14, (1990.)

34. S. J. Brodsky, H. E. Haber, and J. F. Gunion, in *Anti-pp Options for the Supercollider*, Division of Particles and Fields Workshop, Chicago, IL, 1984, edited by J. E. Pilcher and A. R. White (SSC-ANL Report No. 84/01/13, Argonne, IL, 1984), p. 100. S. J. Brodsky, J. C. Collins, S. D. Ellis, J. F. Gunion, and A. H. Mueller, published in Snowmass Summer Study 1984, p. 227.

35. J. Ashman *et al.*, *Phys. Lett.* 202B, 603 (1988) and CERN-EP/88-06 (1988)
M. Arneodo et al., Phys. Lett. 211B, 493 (1988)

36. R. G. Arnold *et al.Phys. Rev. Lett.* 52, 727 (1984) and SLAC-PUB-3257 (1983)

37. J. S. Bell, *Phys. Rev. Lett.* 13, 57 (1964)

38. L. Stodolsky, *Phys. Rev. Lett.* 18, 135 (1967)

39. S. J. Brodsky and J. Pumplin, *Phys. Rev.* 182, 1794 (1969)

40. J. J. Sakurai and D. Schildknecht, *Phys. Lett.* 40B, 121 (1972); *Phys. Lett.* 41B, 489 (1972); *Phys. Lett.* 42B, 216 (1972)

41. R. J. Glauber, in *Lectures in Theoretical Physics*, edited by W. E. Brittin *et al.*(Interscience, New York, 1959), vol. I

42. T. H. Bauer, R. D. Spital, D. R. Yennie and F. M. Pipkin, *Rev. Mod. Phys.* 50, 261 (1978)

43. P. V. Landshoff, J. C. Polkinghorne and R. D. Short, *Nucl. Phys.* B28, 225 (1971)

44. S. J. Brodsky, F. E. Close and J. F. Gunion, *Phys. Rev. D* 5, 1384 (1972)

45. S. J. Brodsky, and H. J. Lu, *Phys. Rev. Lett* 64, 1342 (1990)

46. A. H. Mueller and J. Qiu, *Nucl. Phys.* B268, 427 (1986)
J. Qiu, Nucl. Phys. B291, 746 (1987)

47. See the talks of E. Levin, A. Mueller, and M. Ryskin, this conference.

48. N.N. Nikolaev and V. I. Zakharov, MPI-PAE-PTh-11/90, (1990); Physics Letters 55B 397 (1975); Sov. J. Nucl. Phys. 21, 227 (1975).

49. See M. Ryskin, this conference.